

NUMERICAL SIMULATION OF THE 24 APRIL, 2002 STORM MERGER BETWEEN A LEFT MOVING STORM AND SUPERCELL

Brian F. Jewett¹, Ron W. Przybylinski², and Robert B. Wilhelmson¹

¹Atmospheric Sciences Department & NCSA, University of Illinois

²National Weather Service Forecast Office/NOAA, St. Louis, Missouri

1. INTRODUCTION

There has long been a suspected association between tornadogenesis and storm merging. While the presence of nearby cells can enhance or detract from storm intensity and longevity (see P11.4), the relationship between merging and tornadogenesis is of particular concern for warning meteorologists, considering the short time period possible between merging and touchdown (Lee et al. 2006). This study addresses one such event, through numerical simulations and observations.

Tornadic storms sometimes occur in lines, of which the 3-4 April 1974 outbreak was a notable example (Locatelli et al. 2001). The potential severity of storms in lines can be limited by the nearly two-dimensional forcing in some cases, and depends significantly on cell spacing and line orientation with respect to the vertical shear vector (Rotunno, Klemp and Weisman 1988, hereafter RKW; Bluestein and Weisman, 2000). In cases in which the shear is normal to the line, storm split pairs may interact, reducing the likelihood of steady cells and therefore the line longevity (RKW). However, storm proximity can also lead to intensification (Jewett et al. 2002), and possibly tornadogenesis.

2. OBSERVATIONS

On 24 April 2002, a broken line of severe thunderstorms developed ahead of a cold front advancing NW-SE across Missouri. While

widespread hail events accompanied this storm system, tornado incidence was relatively rare and confined to a narrow region of southeast MO and southern IL (NOAA, 2002). Of interest was one storm in this line which produced a tornado which caused F2 damage along a 9-mile track over southern Madison County Missouri.

The line segments associated with the subsequent tornadic storm first developed near 1900 UTC, in south-central MO (Fig. 1). The NNE-SSE line developed southward with time.

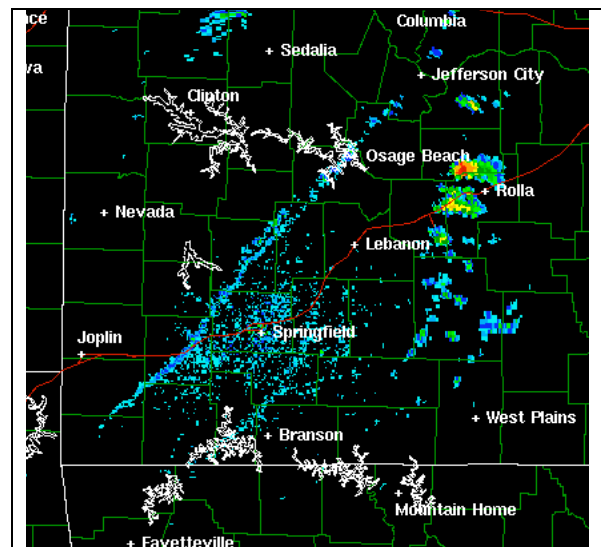


Fig. 1: 1907 UTC reflectivity from SGF, MO.

As the storms moved eastward, two line segments south of St. Louis were noted (Fig. 2). Immediately south of the three northern cells, a storm split occurred, with the left-moving (LM) cell propagating northward towards the third cell in the line segment to its north (Fig. 3). The LM then merged with this cell on its forward flank. A tornado formed 30 minutes later, near 2145z.

¹Corresponding author address:

Dr. Brian F. Jewett - 212 Atmospheric Sciences Bldg
105 S. Gregory St., Urbana IL 61801

Email: bjewett@uiuc.edu

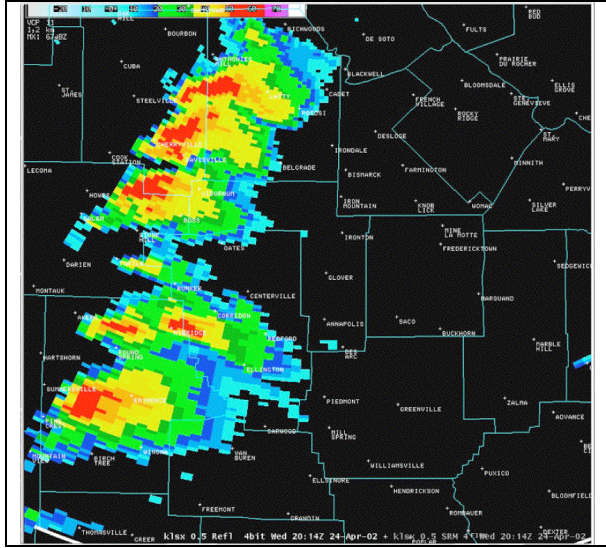


Fig. 2: broken squall line SW of STL (2014z).

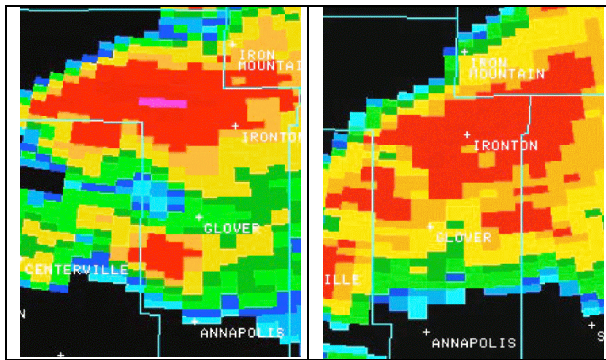


Fig. 3: LM cell approaching storm to its north; WSR-88D reflectivity from 2100 and 2115 UTC.

3. MODELING METHODOLOGY

Sounding data was not available near the time and location of these severe storms. We used results of a 24-hour WRF simulation of this case, initialized with 00z 24 April NCEP Eta analyses. Thermodynamic data was extracted at 19z and, along with wind profiler data from Bloomfield, MO, a sounding was created for use in subsequent idealized (horizontally uniform) experiments. This sounding was characterized by 2800 J kg^{-1} CAPE, 8.5 J kg^{-1} CIN, and a shear vector largely directed WNW-ESE, nearly normal to the line orientation.

The idealized WRF v2.1.2 runs utilized 1-km grid spacing over a 140×120 domain, with 70 stretched vertical levels. The most recent Thompson microphysics parameterization, due for release in WRF v2.2, was employed, along with 1.5 order TKE closure.

Convective initiation was accomplished by using two warm thermals. Splitting occurred in both storms. Cell placement was such that the northern storm's LM exited the domain, while the southern storm left-split cell moved towards the storm to its north. We varied the southern cell's initial θ' and E-W location to alter the properties and location of the LM split cell that would approach the northern storm. WRF was run 4 hours, and data saved each minute.

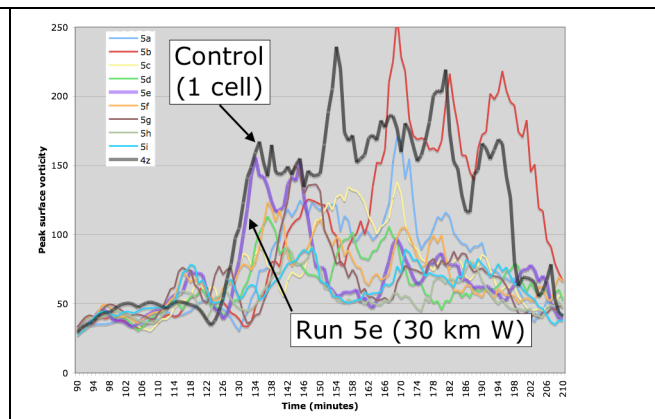
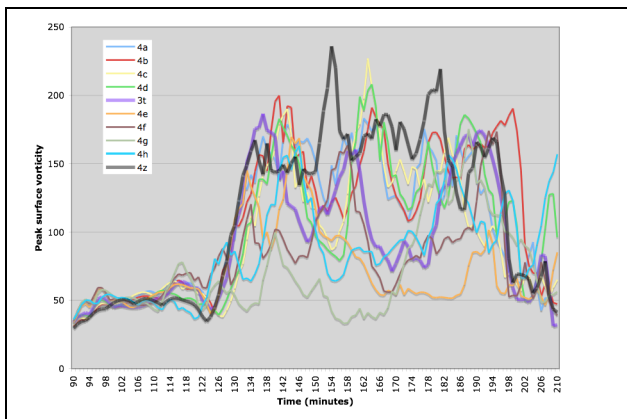


Fig. 4A,B: Peak surface vorticity ($\times 10^{-4} \text{ s}^{-1}$) after 90 minutes for 2° WRF series (left), 2.5° series (right).

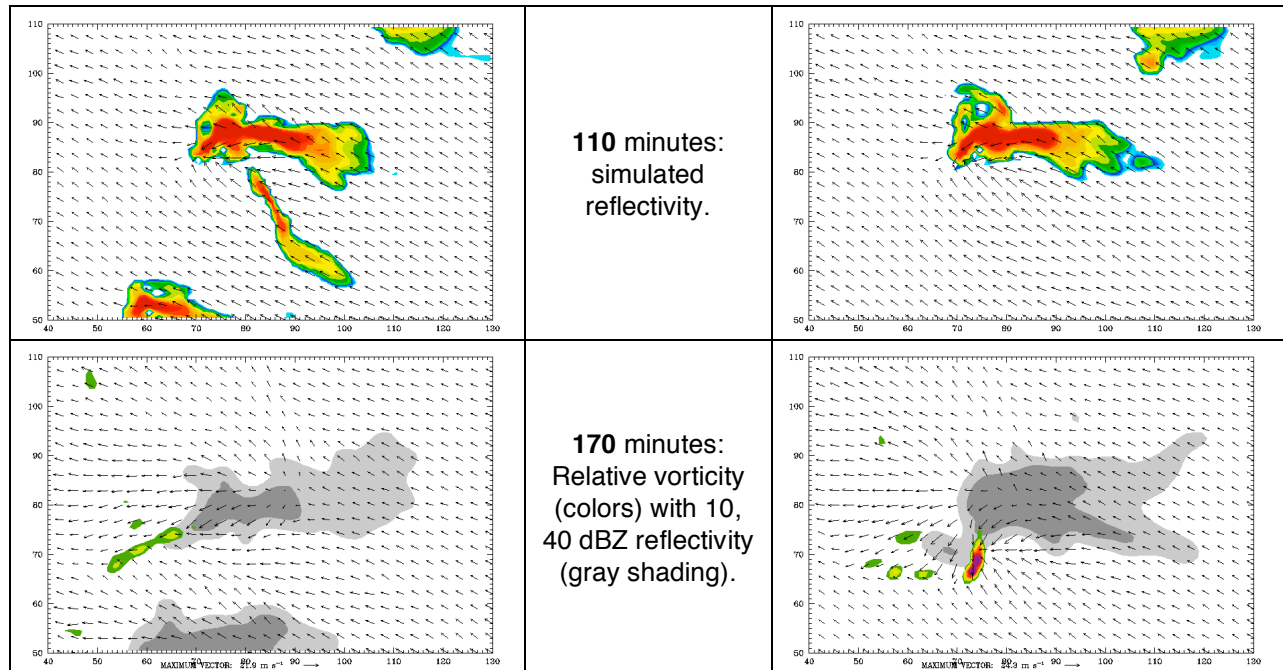


Fig. 5: Evolution of case 5h cells (left) and single-cell control case (right) over a 1 hour period. Note only the northern half of the model domain is shown (so the LM appears, but the southern cell does not).

4. RESULTS

Initial temperature perturbations of 2° , 2.5° , and 3.5°C were used to initiate the southern storm. Larger values resulted in a more vigorous and faster-moving LM cell. For each temperature perturbation, a series of simulations were made in which we varied the E-W location of the southern cell, ranging from 60km west to 15 km east of the primary storm. The LM split cell thus approached the northern storm from the SW, S, or SE as it moved to the NE. Results are summarized for each set of simulations below.

For the 2° simulation set, fairly weak left-split cells emerged to interact with the northern storm. The time series of maximum surface vertical vorticity appears in Fig. 4A. The control case had only one (northern) cell; this is shown in all time series figures with a bold black line. The control run exhibited the highest vorticity, but the overall pattern was similar – vorticity increased most dramatically after storm splitting (of both cells). The time of increased rotation was comparable whether a southern cell (and thus a LM split cell) existed or not. The most

striking differences are (1) intensity – all cells other than the control exhibit a notably unsteady nature, and (2) timing – in many cases the 2-cell case intensification was somewhat delayed relative to the control.

The 2.5° simulation series produced a stronger LM split cell. The appropriate vorticity time series appears in Fig. 4B. Some cases again resemble the control; note the early similarities between the control and case 5e. In others, the development of significant rotation at the surface was delayed. Finally, some cases showed little intensification over the 3.5 hour period shown; this could be attributed to a stronger LM raining into the inflow air bound for the incipient rotation center on the west end of the northern cell. Case 5h was an example of the latter. The LM, which had become quite elongated prior to merging with the primary storm, had a lasting impact on storm structure. After an hour (Fig. 5), the 5h storm was highly linear and quite weak, while the control was going through another period of intensification. In some cases these differences persisted for the lifetime of the modeled storms.

Finally, we address the 3.5° case, which resulted in the strongest split LM cell and the clearest indication of the influence it could have on the primary cell development. Fig. 6 shows the time evolution of the simulations, with three cases and the control highlighted.

A range of responses were noted. When a LM cell approached the northern storm from the southwest, the result was often a very weakened northern storm after merging occurred on its southwest flank. Any reintensification was delayed, as in case *3b* in Fig. 6.

In simulations in which the southern cell (and its LM split cell) were initially placed farther east – such that the LM approached more nearly from the south – the resulting 2-storm behavior changed as well. The initial stages of such cases were again weak, but for a shorter period of time, with notable strengthening thereafter. Many of these cases exhibited reasonably quick motion of the LM cell to the northeast, such that interruption or contamination of the main storm inflow was limited to a shorter period of time. An example of such behavior was case *3e* in Fig. 6. While remaining weaker than the control, it still exhibited a (actually two) periods of heightened rotation. We note also that this behavior was

represented in “nearby” (in parameter space) WRF results, but that sharp changes were sometimes noted between simulations with small changes in the southern storm position. Case *3m*, not highlighted below, placed the initial southern storm only 5 km east of *3e* but behaved quite differently – more like cases discussed below, suggesting a different regime of behavior was present.

When the LM cell approached from the south/southeast, the behavior again changed. While the LM in such cases appeared to merge, or influence, the far-eastern flank of the northern storm, the outflow from the LM cell was apparently strong enough to increase convergence on the south side of the northern storm, leading to an early increase in surface vorticity. In some cases this intensification occurred up to 15-20 minutes before the control case with no LM cell present. *3h* in Fig. 6 was one such case. Beyond the early intensification, many of these storms remained weakened after this early peak, a surprisingly long-term effect considering what appears (in simulated reflectivity animations) to be a “glancing blow” from the left-mover as it merges with or moves beyond the eastern flank of the primary cell.

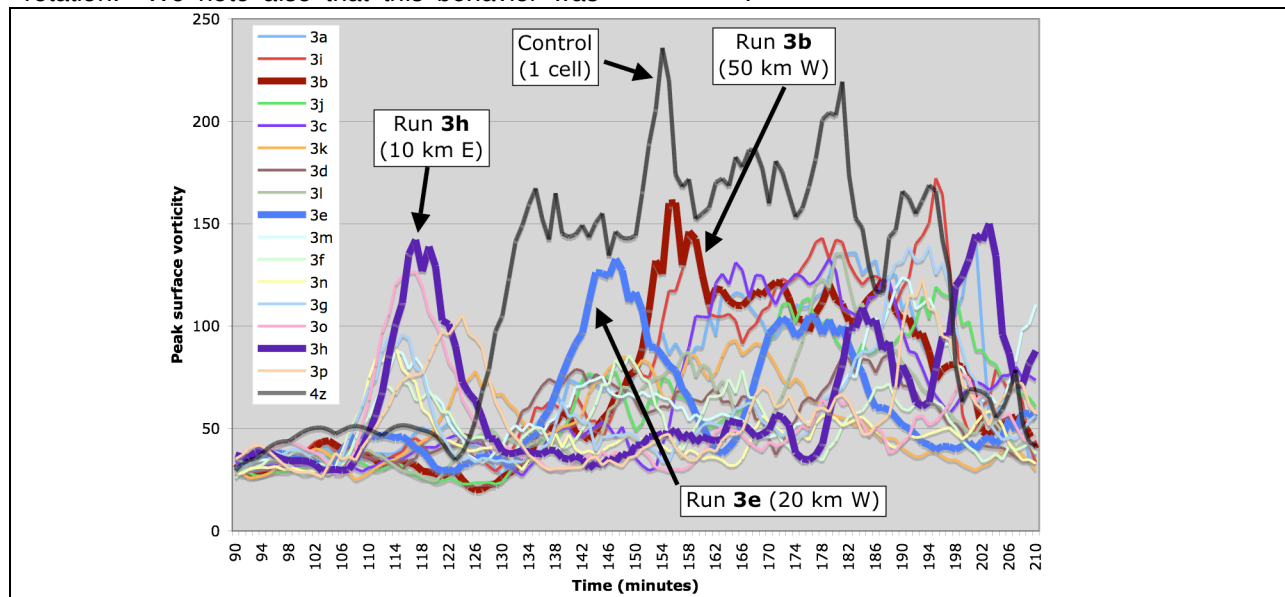


Fig. 6: Peak surface vorticity ($\times 10^{-4} \text{ s}^{-1}$) after 90 minutes for Series 5. Run 5h is purple; control is black.

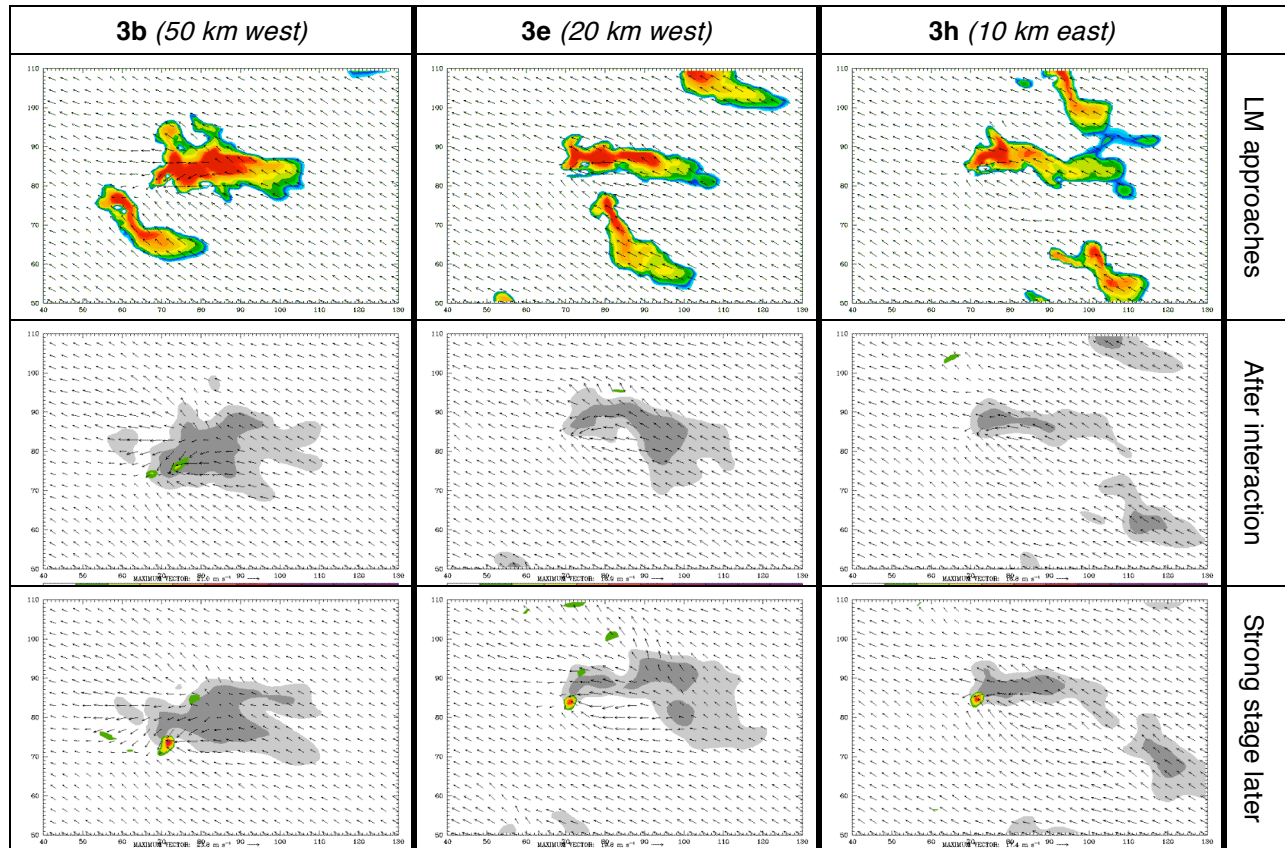


Fig. 7: 3 sets of storms evolve. Top: reflectivity; middle/bottom: vorticity (colors), reflectivity (gray scale) (approx 20 min between rows). Left-right: case 3b (50 km W); case 3e (20 km W), and case 3h (10 km E)

Snapshots from the aforementioned three cases appear in Fig. 7. Note the times chosen here were for similar stages in evolution (i.e. proximity of the LM); this occurred at different times for different LM approach angles, resulting in differences in the “pre-merger” images above. In the top row, the simulated reflectivity is shown as the LM cell approaches the northern storm, while the northern storm’s LM split cell is exiting the north edge of the model domain. In the middle row, merging (or other interaction) has occurred, and the plot has been changed to show surface vorticity, with gray shading indicating the 10 and 40 dBZ regions. 10-20 min later, all cases have exhibited intensification.

5. DISCUSSION

First it should be noted that it is not possible in this type of experiment to create truly identical

initial conditions between cases, apart from the shift in the LM position. The LM appears accelerated northward (presumably due to enhanced inflow into the northern storm) when it approaches from the south or southeast. Structural changes occur as well, limiting the symmetry between cases seen early in the simulations, when the northern storm looks much like the control.

If the time of vorticity intensification is plotted (not shown), the general pattern is one of earlier strengthening for LM cells located farther to the east. The differences between cases are not simply timing, however. Some cases are more likely to reintensify after a shorter delay – this appears true for 3e, when the LM approached from the south. Nearly all cases in which a second cell was present are less steady than the control, for reasons that are not entirely clear.

The rapid and early intensification of rotation in cases such as *3h* is surprising and, given clustering of runs in Fig. 6, apparently in a different regime from merging cases in which the LM approaches from the S or SW.

Also evident in Fig. 6 are many simulations in which little rotation was evident. The negative impact of the influence and/or merging with the LM cell is striking in these cases. Further examination of the inflow properties, trajectories and other analysis are needed to clarify why these storms remained weak, in some cases well after the LM merged or propagated away from the northern storm. Ingesting rain-cooled air is an obvious candidate; dynamic effects are of more interest.

There are several mechanisms that could contribute to intensification of low-level rotation. One is stretching as a result of enhanced low-level convergence. This would likely require a balance between the intensity of the LM outflow and the effect on buoyancy properties of air enroute to the updraft. Another is enhanced θ_e gradients along the southern periphery of the northern storm, potentially increasing horizontal vorticity generation in air subject to tilting later. This could occur, e.g., by enhanced forward-flank rainfall and cooling after merging occurs east of the updraft.

We return now to the 24 April 2002 case. The storms modeled here evolve in notably different ways, which is not unexpected in single-sounding simulations. Nonetheless, a wide variety of responses to merging/proximity of the LM are seen, depending on the approach angle as well as the properties of the LM cell itself. Experiments such as case *3h* are indicative of the rapid intensification (relative to control) that is possible. Future work will include higher resolution simulations and trajectory analysis to better understand the short- and long-term effects of cell merging on storm intensity and longevity.

6. ACKNOWLEDGEMENTS

The convective storms work is supported by NSF under grant ATM-0449753. Computing and other support was provided by the National Center for Supercomputing Applications.

7. REFERENCES

- Bluestein, H. B., and M. L. Weisman, 2000: The interaction of numerically simulated supercells initiated along lines. *Mon. Wea. Rev.*, **128**, 3128-3149.
- Jewett, B. F., R. B. Wilhelmson, and B. D. Lee, 2002: Numerical simulation of cell interaction. *Preprints, 21st Conf. on Severe Local Storms*, San Antonio, Amer. Meteor. Soc., 353-356.
- Lee, B. D., B. F. Jewett and R. B. Wilhelmson, 2006: The 19 April 1996 Illinois tornado outbreak. Part I: Cell initiation, evolution and supercell isolation. *Wea. Forecasting*, **21**, 433-448.
- _____, _____, and _____, 2006: The 19 April 1996 Illinois tornado outbreak. Part II: Cell mergers and associated tornado incidence. *Wea. Forecasting*, **21**, 449-464.
- Locatelli, J. D., M. T. Stoelinga, and P. V. Hobbs, 2001: A new look at the super outbreak of tornadoes on 3-4 April 1974. *Mon. Wea. Rev.*, **130**, 1633-1651.
- NOAA Storm Prediction Center, 2002: SPC storm reports. Available at www.spc.noaa.gov.
- Rotunno, R., J. B. Klemp, and M. L. Weisman, 1988: A theory for strong, long lived squall lines. *J. Atmos. Sci.*, **45**, 463-485.